

JET-P(93)101

K. Thomsen, B. Balet, D.J. Campbell, C.D. Challis, J.G. Cordey,  
N. Deliyankis, J.J. Ellis, C.M. Greenfield, N. Hawkes,  
D.G. Muir, D.P. O'Brien, R. Reichle, D. Stork, P. Stubberfield,  
P.R. Thomas and the JET Team

# Global and Local Confinement Analysis of JET's VH-Mode Pulses

“This document contains JET information in a form not yet suitable for publication. The report has been prepared primarily for discussion and information within the JET Project and the Associations. It must not be quoted in publications or in Abstract Journals. External distribution requires approval from the Publications Officer, JET Joint Undertaking, Abingdon, Oxon, OX14 3EA, UK”.

“Enquiries about Copyright and reproduction should be addressed to the Publications Officer, EFDA, Culham Science Centre, Abingdon, Oxon, OX14 3DB, UK.”

The contents of this preprint and all other JET EFDA Preprints and Conference Papers are available to view online free at [www.iop.org/Jet](http://www.iop.org/Jet). This site has full search facilities and e-mail alert options. The diagrams contained within the PDFs on this site are hyperlinked from the year 1996 onwards.

# Global and Local Confinement Analysis of JET's VH-Mode Pulses

K. Thomsen, B. Balet, D.J. Campbell, C.D. Challis, J.G. Cordey,  
N. Deliyannis, J.J. Ellis, C.M. Greenfield<sup>1</sup>, N. Hawkes<sup>2</sup>  
D.G. Muir, D.P. O'Brien, R. Reichle, D. Stork, P. Stubberfield,  
P.R. Thomas and the JET Team

*JET-Joint Undertaking, Culham Science Centre, OX14 3DB, Abingdon, UK*

<sup>1</sup>*General Atomics, San Diego, California, USA.*

<sup>2</sup>*Culham Laboratory, UKAEA/Euratom Fusion Association, Abingdon, Oxon, OX14 3DB, UK.*

Preprint of a paper to be submitted for publication in  
Plasma Physics and Controlled Fusion (special issue).



## ABSTRACT

Plasmas with the energy confinement time enhanced by a factor 1.4 to 2.1 over the ITER93H-P H-mode scaling expression have been obtained in 3 different H-mode regimes (excluding pellet injection) in JET. The phase of enhanced confinement has strong similarities with the VH-mode observed in DIII-D in all 3 cases. The JET data clearly show VH-mode confinement increasing with plasma current and degrading with loss power.

## I. INTRODUCTION

The thermal energy confinement time obtained in most H-mode discharges in JET lies within 1 - 2 standard deviations of existing H-mode confinement scaling expressions. However, in 3 discharge types the thermal confinement is enhanced over both the JET/DIII-D<sup>(1)</sup> and the ITER93H-P<sup>(2,3)</sup> ELM-free H-mode thermal confinement scaling expressions by a factor  $> 1.4$ . The enhanced confinement phase (relative to the scalings) in these discharges has been studied extensively <sup>(4,5,6,7)</sup> and compared with the VH-mode <sup>(12)</sup> observed in DIII-D <sup>(8,9,10,11)</sup>. Although there are some differences between enhanced confinement H-modes in JET and VH-modes in DIII-D the similarities are so strong that the JET enhanced confinement H-modes are now regarded as VH-modes.

This paper is a continuation of the work already published <sup>(9)</sup> on describing the characteristics of the JET VH-mode data. However, the data have been selected differently. First the selection criterion  $\tau_E$  (diamagnetic)  $\geq 1.4 \times$  ITER93H-P scaling was applied to the entire JET H-mode dataset. This was followed by an elimination of all data featuring pellets and data with  $\tau_E \gg \tau_{\text{thermal}}$ . Data from 50 JET discharges survived this selection procedure and they could be divided into 3 types of discharges which have been labelled in this paper as: 1) High  $\beta_p$  1 MA discharges (11 shots); 2) Hot ion 3 MA discharges (36 shots) and 3) Old 1988 3 MA discharges (3 shots). In Section 2 the experimental conditions and typical temporal evolution of the 3 types of discharges are described. The similarities with the DIII-D VH-mode are discussed in Section 3. The trends of the confinement time in the selected dataset are examined in Section IV. Finally the results are summarised in Section V.

## II. DISCHARGE CHARACTERISTICS

Fig. 1 shows the diamagnetic energy confinement time  $\tau_E$  against the loss power  $P-dW/dt$  of the data selected according to the selection procedure outlined in the introduction. The data can be divided into 3 types of discharges. Each group of data shows a clear enhancement with respect to the JET/DIII-D ELM free thermal H-mode scaling expression shown by dashed lines for 1 and 3 MA. For the moment a good thermal confinement estimate is not available for all the data. Where a comparison of  $\tau_E$  with  $\tau_{\text{thermal}}$  estimated by TRANSP is possible the agreement between the two estimates are within 10-20% and the estimates of fast ion content obtained with the PION and PENCIL codes respectively, agree with those of TRANSP. For the shots without TRANSP data available the PION and PENCIL estimates were used to judge that  $\tau_E \approx \tau_{\text{thermal}}$ . It may therefore be justified to use  $\tau_E$  instead of  $\tau_{\text{thermal}}$ .

The main characteristics of the 3 types of discharges are as follows:

- a) **High  $\beta_p$  1 MA discharge (11 shots).** These Double Null (DN) X-point discharges with a plasma current of 1 MA were produced during the 1991/92 experimental campaign when the torus was well conditioned due to Be evaporation. The toroidal magnetic field at the geometric centre was either 3 or 3.2T giving a  $q_{95}$  in the range 12-14. The low target density of  $\langle n_e \rangle \approx 1 \times 10^{19} \text{ m}^{-3}$  was well below the density limit at 1 MA. The discharges were heated by up to 8 MW of ICRF heating and strong gas puffing was used to ensure good ICRF coupling. Further details of these experiments have been published in Ref. (6).
- b) **Hot ion 3 MA discharges (36 shots).** These X-point discharges with a plasma current of 3 MA were also part of the 1991/92 experiments when the torus was well conditioned by the use of Be evaporation. The configuration was either in DN or Single Null (SN) X-point. In SN configuration the ion  $\nabla B$  drift direction was either pointing towards or away from the X-point. The range in toroidal field was 1.9 - 3.3T giving a range in  $q_{95}$  of 2.5 - 4.8. The hot ion type of plasmas ( $T_i \gg T_e$ ) was achieved with strong NBI heating but also ICRH was applied in some of the shots. A low to moderate target density  $\langle n_e \rangle \approx 2 \times 10^{19} \text{ m}^{-3}$  created the hot ion condition. Neutral beam heating was also required at X-point formation to prevent locked modes. Further details of these pulses have been published in Ref. (7,13).

- c) **Old 1988 3 MA discharges (3 shots).** These SN X-point discharges with the ion  $\nabla B$  drift direction towards the X-point with a plasma current of 3 MA were obtained in 1988 experiments when Helium discharge cleaning was used to condition the torus. The toroidal field at the geometric centre of the plasma was 3.4T and  $q_{95} \approx 5-6$ . NBI heating produced so called medium density H-modes from target densities  $\langle n_e \rangle \lesssim 2 \times 10^{19} \text{ m}^{-3}$ . Further details of these shots have been published in Ref. (4,5).

The temporal behaviour of the enhancement factor  $H(\text{ITER93H-P}) = \tau_{\text{thermal}}^{\text{TRANSP}} / \text{ITER93H-P}$  scaling for a shot from each of the 3 groups above which have been analysed with the TRANSP code is shown in Fig. 2 together with traces of  $D_{\alpha}$ -emission and auxiliary heating power. It can be seen that the enhanced confinement phase is usually preceded by an ELMy phase. The termination of the enhanced confinement phase in the 3 types of shots have been studied in detail elsewhere (5,6,13) and will not be discussed in this paper.

### III. COMPARISON WITH THE VH-MODE IN DIII-D(9,12,14)

The disappearance of momentum transfer events (MTEs) is observed in DIII-D when the discharge enters the VH-mode phase. In this phase the thermal confinement is significantly better than that given by the JET/DIII-D scaling. The improved confinement in the VH-mode corresponds to a broadening of the region of high density and temperature gradients which develop near the edge during the H-mode. The single fluid heat diffusivity  $\chi_{\text{eff}}$  decreases during the entire phase and the  $\chi_{\text{eff}}$  profile becomes flatter and is reduced over most of the plasma cross section compared to that of a normal H-mode. The improved confinement is believed to be associated with a broadening of the radial electric field shear due to an enhanced toroidal rotation shear in the confinement region of the plasma. A large bootstrap current density develops near the edge and in this region access to the 2nd stable regime for ideal ballooning modes is achieved. In JET MTEs have not been observed. Instead ELMs are usually observed before the enhanced confinement phase (see Fig. 2). In this phase the thermal confinement is significantly improved compared to both the JET/DIII-D (see Fig. 1) and ITER93H-P (see Fig. 2) scaling expressions. In JET the poloidal rotation is determined to be zero within errors in L- and H-mode (15). In normal H-modes the electric field at the edge is due to the density gradient. Unfortunately no poloidal rotation data are available for the selected dataset and so no statement can be made about the poloidal rotation in the VH-mode phase. In the enhanced

confinement phase the effective heat diffusivity  $\chi_{\text{eff}}$  is flatter and lower compared with normal H-modes in the high  $\beta_p$  and 1988 shots (6,5). In the hot ion pulses the ion heat diffusivity shows the same behaviour (7). This improvement in confinement is not accompanied by an enhancement of toroidal rotation shear in all shots. In high  $\beta_p$  ICRH heated shots and the 1988 shots the toroidal rotation shear even seems to decrease as is shown in Figure 3. However, the shots from the dataset which have been analysed with TRANSP all develop a large bootstrap current density near the edge. For a few of the shots reflectometer electron density measurements at the edge are available. For these it has been possible to conclude that there is access to the 2nd stable regime for ideal ballooning modes (8,10). In these shots the period of access coincides with the period of enhanced confinement. However it is not possible from the measurements to determine if the access to the 2nd stable regime is a cause or a consequence of the enhanced confinement phase.

It is clear from the above that the DIII-D VH-mode and the JET VH-mode are very similar with one exception, that the poloidal and toroidal rotation in JET plasmas do not play such an important role as are seen in DIII-D plasmas.

#### IV. VH-MODE CONFINEMENT TRENDS IN JET

In this paper the enhanced confinement data are compared with two thermal ELM free H-mode confinement scaling expressions. These are the JET/DIII-D and ITER93H-P scalings which are listed below

$$\text{JET/DIII-D} : \quad 0.106 I^{1.03} R^{1.48} / P^{0.5}$$

$$\text{ITER93H-P} : \quad 0.036 I^{1.06} n^{1.17} B^{0.32} R^{1.9} a^{-1.11} \kappa^{0.66} M^{0.41} / P^{0.67}$$

In the above expressions the units are MA for plasma current  $I$ , m for major and minor radius  $R$  and  $a$ , T for toroidal field  $B$ ,  $10^{19} \text{ m}^{-3}$  for line average electron density  $n$  and MW for loss power  $P$ . The effective mass number is denoted by  $M$  and  $k$  is the elongation. The enhancement factors  $H$  (JET/DIII-D) and  $H(\text{ITER93H-P})$  used in this paper are defined as the  $\tau_E$ 's of Fig. 2 divided by the values given by the above scaling expressions, respectively. Fig. 4 shows the variation of  $H(\text{JET/DIII-D})$  and  $H(\text{ITER93H-P})$  versus confinement time  $\tau_E$  for the selected dataset. It is clear from these figures that the observed enhancements with respect to ITER93H-P are smaller than those with respect to the JET/DIII-D



scaling. This is not surprising since the JET/DIII-D scaling was established for a JET - DIII-D dataset in which  $B$ ,  $k$  and  $M$  were the same in the two tokamaks whereas this restriction does not apply to the ITER93H-P scaling. It is interesting to note that the 1988 data were included in the dataset used for the ITER93H-P scaling and that the confinement of this data are still outside 2 standard deviations from the scaling.

In Fig. 5 the enhancement factor  $H(\text{ITER93H-P})$  is shown against the variation of normalised beta poloidal  $\epsilon\beta_p$  ( $\epsilon$  is inverse aspect ratio) and normalised beta toroidal  $\beta_N = \beta_T/(I/aB)$ . The  $\beta_p$  has been estimated by the Shafranov  $\beta_I$  as calculated by the EFITJ code whereas the  $\beta_T$  is estimated by  $(2/3 W_{\text{dia}}/\text{Volume})/(B^2/2\mu_0)$ . From the figure it is seen that the enhancement factor increases with  $\epsilon\beta_p$  for the 1 MA data but when this data are combined with the 3 MA data the dependence on  $\epsilon\beta_p$  disappears. Likewise the enhancement factor increases with  $\beta_N$  for the 3 MA data. This dependence also disappears when the data is looked at as a whole. It can also be seen that similar values of  $\beta_N$  have been achieved in the 1 and 3 MA discharges.

Finally some remarks on the observed trends of the confinement time of this dataset with the plasma parameters usually used in scaling expressions. It is clear from Fig. 1 that  $\tau_E$  improves with plasma current and degrades with loss power. If it is assumed that the current and power dependencies are similar to those of the ITER93H-P scaling (reasonable assumption for this dataset) then the variation of  $\tau_E$  with  $I$  and  $P$  can be removed and trends with other parameters may be identified. Fig. 6 shows the result of this procedure. Here  $\tau_E(\text{s}) P(\text{MW})^{.67}/I(\text{MA})$  is shown against the variation of toroidal field and line average density. The figure indicates that the confinement time improves with toroidal field and density.

The dependencies on elongation (range 1.6 - 1.85), triangularity (range 0.4 - 0.7) and internal inductance  $\ell_i$  (range 0.8 - 1.3) are less clear and so no conclusion can be reached on these dependencies.

## V. SUMMARY

An enhanced confinement phase compared to normal H-mode behaviour has been achieved in 3 different types of discharge in JET (excluding PEP H-modes). The 3 types are: a) High  $\beta_p$  ICRH heated discharges in which the electron temperature  $T_e$  is greater than the ion temperature  $T_i$ ; b) Hot ion NBI (or NBI

with modest ICRH) heated discharges in which  $T_i \gg T_e$  and c) Some NBI heated medium density H-mode discharges in which  $T_e \sim T_i$ . A necessary condition for achieving this enhanced confinement phase seems to be a well conditioned torus. The enhanced confinement phase in all 3 types have strong similarities with the enhanced confinement phase in DIII-D labelled VH-mode. Hence this phase has also been labelled VH-mode. In DIII-D there is a clear correlation between increased toroidal rotation shear and the improvement in confinement. This is not the case for the JET data.

The confinement time of the JET VH-modes are more than 2 standard deviations from the ITER93H-P scaling. It has not been possible to identify any global scaling parameter which can unify the H- and VH-mode datasets. However, it can be clearly seen from the JET VH-mode dataset that the confinement increases with current and degrades with loss power. In addition there is some indication of an improvement with toroidal field and plasma density.

## REFERENCES

- 1) Schissel, D.P., DeBoo, J.C., Burrell, K.H., et al., Nucl. Fusion **31** (1991) 93.
- 2) Schissel, D.P., and H-mode database working group, EPS Lisboa Conf., Portugal (1993).
- 3) Thomsen, K., Campbell, D.J., Cordey, J.G., et al., Submitted to Nucl. Fusion.
- 4) Keilhacker, M., and the JET Team, Plasma Physics and Controlled Fusion Research (Proc. 12th Int. Conf., Nice, 1988), Paper IAEA-CN-50/A-III-2, IAEA, Vienna.
- 5) Watkins, M.L., Balet, B., Bhatnagar, V.P., et al., Plasma Phys. and Controlled Fusion **31** (1989) 1713.
- 6) Challis, C.D., Hender, T.C., O'Rourke, J., et al., Nucl. Fusion **33** 1097.
- 7) Balet, B., Stubberfield, P.M., Borba, D., et al., to be published in Nuclear Fusion.
- 8) O'Brien, D.P., Balet, B., Deliyannis, N., et al., 1993 Sherwood Fusion Theory Conference, Newport Rhode Island, USA.
- 9) Greenfield, C.M., Balet, B., Burrell, K.H., et al., JET-P(93) 75 to be published in Plasma Phys and Controlled Fusion.
- 10) Delyanakis, N., O'Brien, D.P., Balet, B., et al., Submitted to Plasma Phys. and Controlled Fusion.
- 11) Thomas, P.R., and the JET Team, APS St. Louis, USA, 1993.
- 12) Jackson, G.L., Winter, J., Taylor, T.S., et al., Phys. Rev. Lett. **67** (1991) 3098.

- 13) Reichle, R., Campbell, D.J., Ali-Arshad, S., et al., to be submitted to Nucl. Fusion.
- 14) Staebler, G.M., Hinton, F.L., Wiley, J.G., et al., GA-A21278, September 1993.
- 15) Hawkes, N., EPS Lisboa Conf., Portugal (1993).

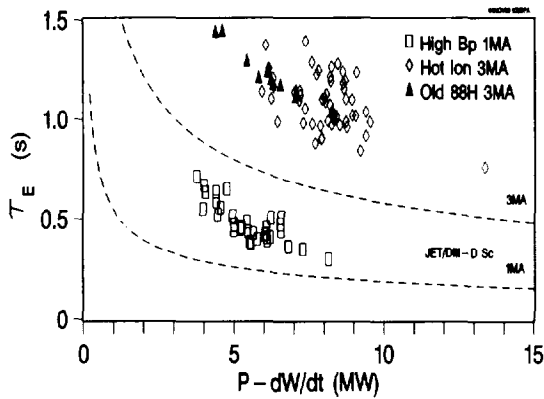


Fig. 1 Energy confinement time (diamagnetic) of the 3 types of discharges versus loss power. The 1 MA and 3 MA predictions of the JET/DIII-D scaling are shown by the dashed lines.

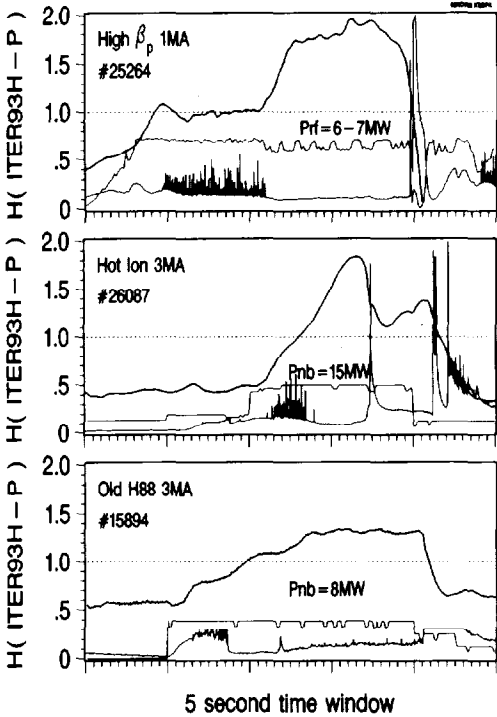


Fig. 2 Time traces of  $D_{\alpha}$  emission, auxiliary power and the enhancement factor  $H(ITER93H-P)$  as defined in the text for a representative shot from each of the 3 types of discharges. The selected time windows are #25264: 49-54 secs; #26087: 50-55 secs and #15894: 53-58 secs.

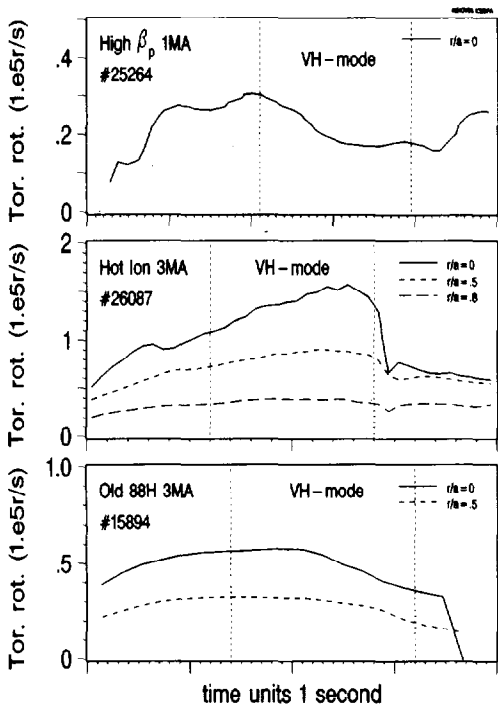


Fig. 3 Time traces of toroidal angular rotation frequency as measured by X-ray crystal spectrometer (#25264) and charge exchange spectroscopy (#26087 #15894). Top) shows central toroidal rotation for #25264. Middle) Toroidal rotation at 3 different radii for #26087 and Bottom) toroidal rotation at 2 different radial positions for #15894. The duration of the enhanced confinement phase is indicated with vertical dashed lines for each shot.

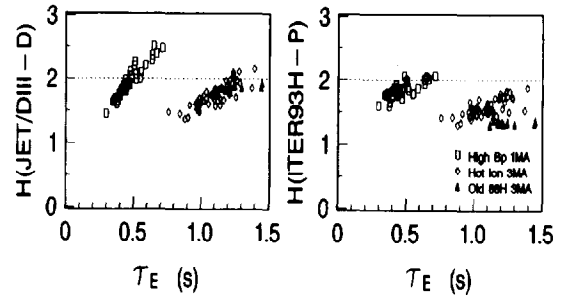


Fig. 4 Measured enhancement factors  $H(JET/DIII-D)$  and  $H(ITER93H-P)$  as defined in the text versus corresponding energy confinement time (diamagnetic).

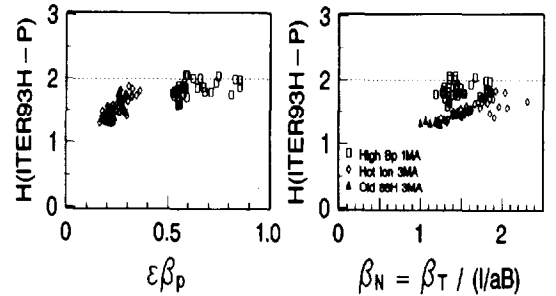


Fig. 5 Measured enhancement factor  $H(ITER93H-P)$  as defined in the text versus  $\epsilon\beta_p$  and  $\beta_N$ .

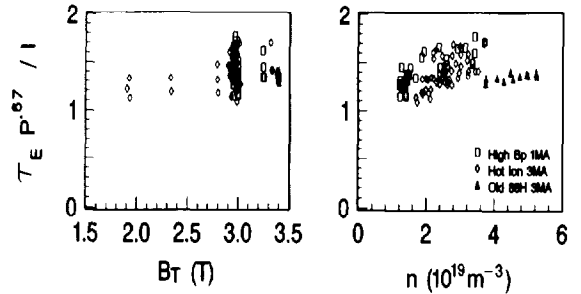


Fig. 6 Normalised confinement time (diamagnetic)  $\tau_E(s) P (MW)^{0.7} / I(MA)$  versus toroidal magnetic field  $B_T$  and line average density  $n$ .